Journal of Engineering and Development, Vol. 18, No.6, November 2014, ISSN 1813- 7822

Flaw Evaluation in Reinforced Concrete Slabs Using Impact Acoustics Method

Asst. Lecturer Wissam Kadhum Al-saraj
Al-Mustansiriyah University, Engineering College, Civil Department

Abstract :

In this study, Impact Acoustics parameters obtained from received sound generated by impact on reinforced concrete slab surface were investigated to develop an evaluation system of flaws in concrete. As Impact Acoustics parameters, frequency distribution was employed. In addition to the experiment, three dimensional FEM analysis was carried out to understand the theoretical background of parameters. The results of FEM analysis showed good agreement with experimental ones. From analytical and experimental results, it was likely possible to estimate flaw size using the relation between the resonance frequencies of impact sounds and flaws diameter.

Key words: Impact, FEM, Acoustics, Effective Time, Crack Width

تقيم الخلل في الألواح الخرسانية المسلحة باستخدام طريقة التأثيرات الصوتية

م.م. وسام كاظم السراج
الجامعة المستنصرية – كلية الهندسة – قسم الهندسة المدنية

الخلاصة

في هذه الدراسة،تم بحث متغيرات الصوت الناتجة من الصوت المستلم المولد بتأثير الصدم على سطح سقف خرساني مسلح لتطوير نظام تقييم الشقوق في الخرسانة. تم توظيف توزيع التردد كما هو في متغيرات الصوت بالإضافة الى التجارب،تم تنفيذ تحليل ثلاثي الإبعاد بطريقة العناصر المحددة لفهم الخلفية النظرية للمتغيرات. بينت نتائج التحليل . مطابقة جيدة مع النتائج التجريبية من النتائج التحليلية والتجريبية، يمكن تخمين حجم الشقوق باستعمال العلاقة بين ترددات رنين التأثير وعرض الشقوق.

Introduction

Tapping methods that receive sounds with human ears have been used in practice to inspect the concrete linings of railway tunnels [1]. However, such methods completely depend on the detection of "unclear sounds" to identify internal flaws.

Evaluation by human ears is greatly affected by the experiences and subjectivity of inspectors.

In order to solve these problems, methods using acoustic device such as microphone to receive sounds and to analyze the waveforms have been studied. The name "Impact Acoustics

Methods" is introduced as a definition of such type of methods in a committee report [2] by Japan Concrete Institute.

This study investigates the Impact Acoustics Methods that can quantitatively identify the sizes of internal flaws and their depths from the surface using the frequency distributions. Experiments were conducted using concrete specimens with an artificial flaws inside, which are represented by voids or demolitions inside concrete.

Numerical analysis of the three-dimensional finite element method (FEM) were also conducted to analyze the relationship between frequency distribution and flaw information. The frequency distributions were compared between concrete sections with and without flaws. The displacements of the concrete surface were monitored using an accelerometer to investigate the phenomena involved in impact acoustics.

Outline of Experiments

Materials

An ordinary Portland cement (type I) was used in this study. The chemical analysis and physical tests results conformed to the Iraqi standard specification IQS:No.5/1984[3]. A fine aggregate of Al-Ukhaider natural sand passing from sieve size of 4.47mm was used for concrete mixes. Results indicate that the fine aggregates used are within the requirement of Iraqi standard specification IQS:No.45/1984[4]. Maximum size coarse aggregate of 10mm was used. Gradation of this crushed river gravel coarse aggregate conforms to the Iraqi standard specification IQS:No.45/1984[4].

The yield strength of steel reinforcement is determined and the average result is 350MPa.

The superplasticizer used in this study was Glenium51, which is free from chlorides and complies with ASTM-C494 type A and F. Glenium51 is compatible with all Portland cements that meet recognized international standards[5].

Molds

The molds used for casting the slab specimens were wood molds. Each mold consists of four movable sides without abed. The sides were fixed together by nails. Five types of molds dimensions were used.

Casting

The concrete was mixed for about three minutes by a horizontal rotary mixer of 0.19m3 capacity. The specimens are then cast in to three layers; each of which are compacted by a Table vibrator. Three (150*150*150mm) concrete cubes were cast with each mix to determine the corresponding compressive strength.

Curing

After casting, the specimens were covered with a nylon sheet to prevent evaporation of water. After 24 hours, the specimens were stripped from the moulds.

Then, cured at the laboratory conditions. To prevent the loss of moisture during curing, specimens were covered with burlap kept continuously wet. One of the three concrete cubes was placed with each specimen to ensure no difference in the corresponding compressive strength with either cube.

Specimens

To evaluate frequency distributions, concrete slab specimens (length: 4000 mm, width: 2000 mm, thickness: 200 mm) that contained of a disk shaped artificial flaws (thickness: 5 mm) were prepared. Photo. 1 shows the details of the specimen used in this study. The mixture proportions and mechanical properties of concrete are shown in **Table (1)**. This size was likely to be large enough to not be affected by elastic wave reflection from the sides. The diameters of artificial flaws were 50, 100, 150, 200, 300 and 500 mm. The depths of the flaws were 30,50,70 and 100 mm from the surface. Flaws were arranged as shown in Photo. 2, and **Figure (1)**. The surfaces of the specimens other than the flaw embedded portion are hereinafter referred to as "the sound portions".

Table 1: Mixture proportions and mechanical properties of concrete.

W/C %	W/B %	Unit weight kg/m^3						Compressive Strength N/mm^2	Ultrasonic Velocity m/s	Dynamic Modulus of Elasticity GPa
		W	C[1)]	F[2)]	S	G	Ad[3)]			
50.0	33.5	175	350	173	817	841	6.8	96.4	4500	41.9

1) normal Portland cement
2) Blast furnace slag powder
3) Water reducing agent
4) Calculated by ultrasonic velocity

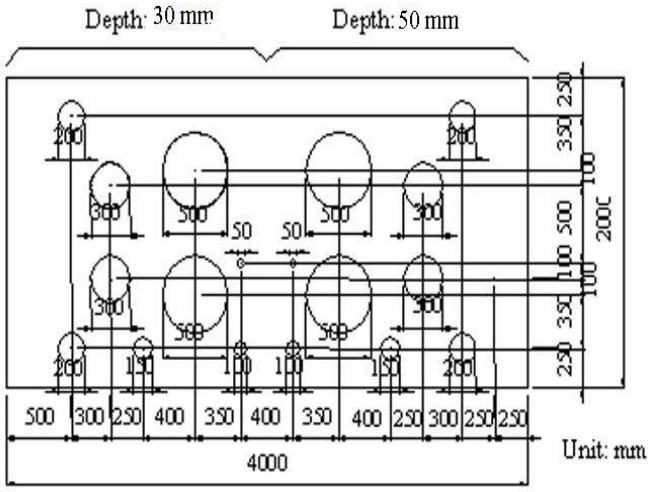

Fig .(1) Location of flaws inside the concrete specimens

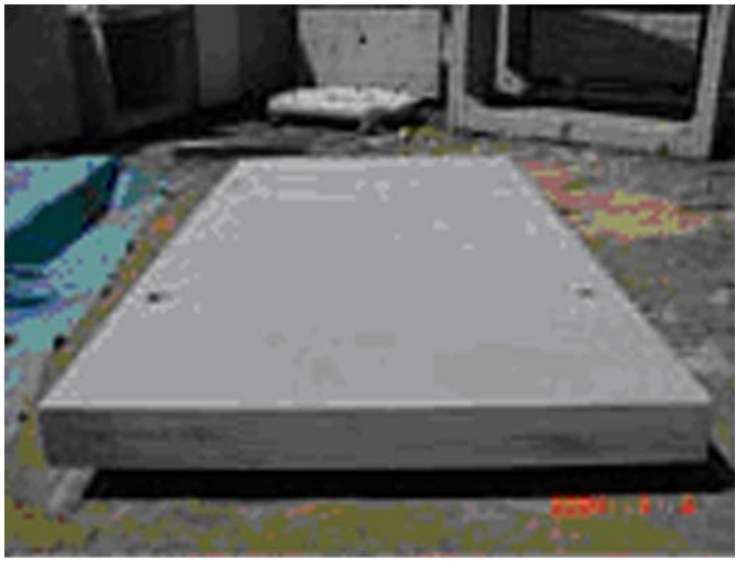

Photo .(1) Concrete slab specimen

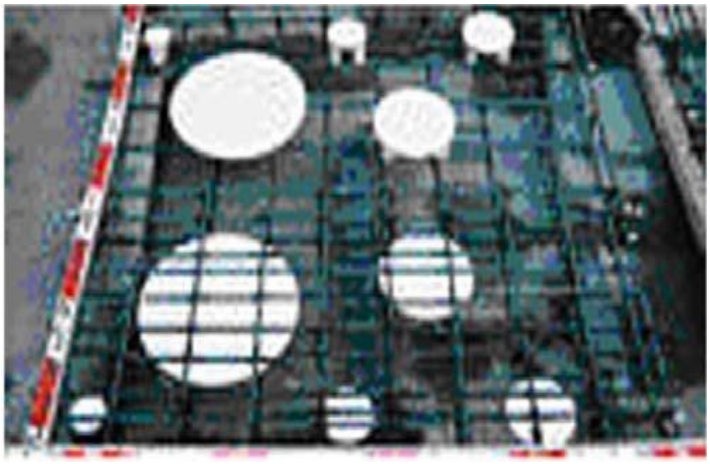

Photo .(2) Arrangement of flaws

Impact method

Elastic wave was induced by impacting the surface of concrete using steel ball drop. Drop height was set at 100 mm from the concrete surface. The diameter of steel ball was 19.05mm. Impact point was at the center of the concrete upper side of the embedded flaws as shown in Photo (3).

Elastic wave measurement

A condenser microphone (which has a flat sensitivity at 20 Hz to 30 kHz) was used to measure the radiating sounds during impact application. Displacement of the concrete surface was monitored using an accelerometer (frequency range: 0.1 to 45 kHz). The accelerometer was attached 50 mm away from the impact point and microphone was positioned 100 mm above the point where the accelerometer was attached. The waveforms received by the microphone and the accelerometer were transmitted through an amplifier and A/D converter to a personal computer. The frequency distributions were then derived by fast Fourier transform (FFT). Test setup for the measurement is shown in photo 3.

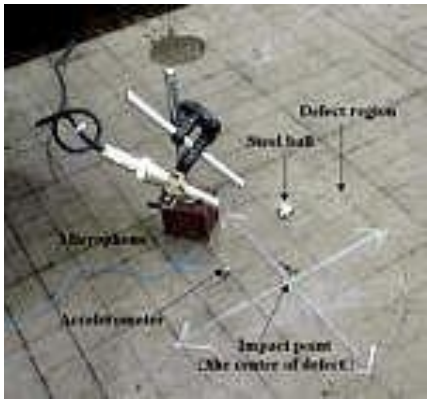

Photo .(3) Test setup.

Outline of FEM Analysis

An analytical investigation using a general purpose program code (LS-DYNA). **Figure (2)** shows the analytical model used in this study. Concrete part upper side of flaw was modeled as a disc shaped plate. Concrete was assumed to be an elastic body (density: 2.3 x 103 kg/m3, elastic modulus: 42 GPa, Poisson's ratio: 0.2), and all degree of freedom of the disc plate base was constrained in the analysis. Load was input as a wave shown in **Figure (3)** to the center of the model. The duration of input *Tc* was derived using the following equation [6]:

$$T_c = 0.0043 \ D \qquad (1)$$

where, *D* is the diameter of the steel ball (m). From Equation (1), the duration of impact to be used for the analysis was determined to be 80μs. The load F_{max} applied to concrete by dropping a steel ball was calculated using the following equation:

$$F_{max} = \frac{m\ (2gh)^{0.3}}{0.637\ T_L} \qquad (2)$$

where, *m* is the mass (kg) of the steel ball, *h* is the height (m) from which the ball was dropped, and *g* is the gravitational acceleration (m/s2). In this analysis, F_{max} was 0.88 kN.

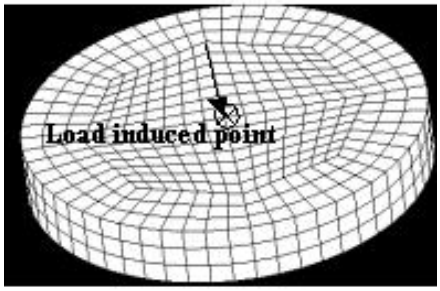

Fig .(2) Model for analysis

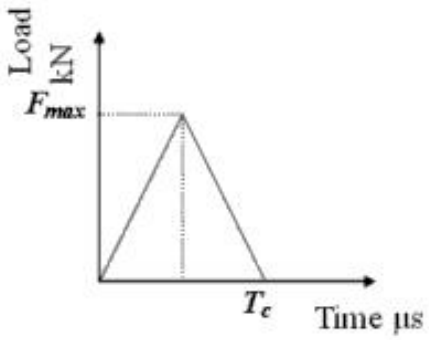

Fig .(3) Input waveform.

Results and Discussions

Waveforms

The waveforms measured by microphone, accelerometer and calculated by FEM are shown in Figure (4) (diameter of defect: 200 mm, depth: 30 mm) and Figure (5) (diameter of defect: 200 mm, depth: 70 mm) respectively. Waveforms monitored in sound portion are also shown in Figure6 for the comparison.

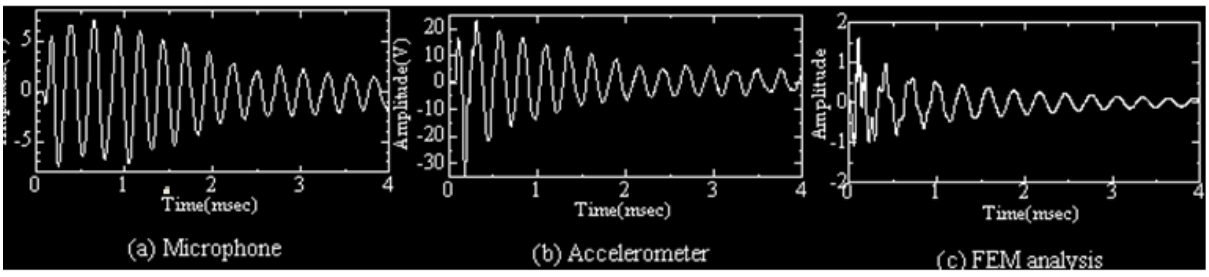

Fig .(5) waveforms (diameter: 200 mm, depth: 30 mm).

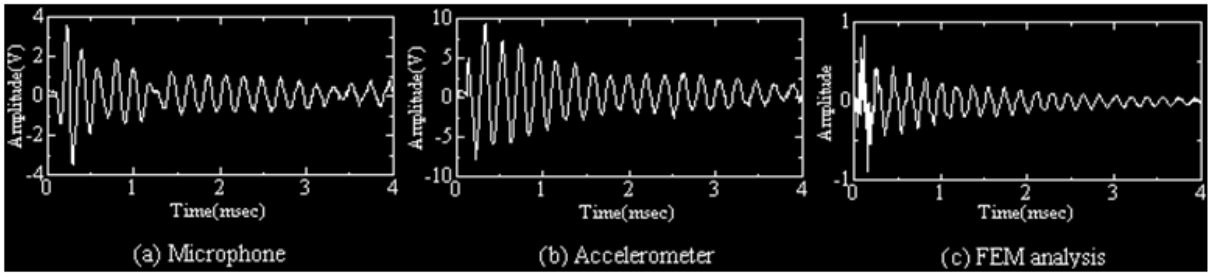

Fig .(5) waveforms (diameter: 200 mm, depth: 70 mm).

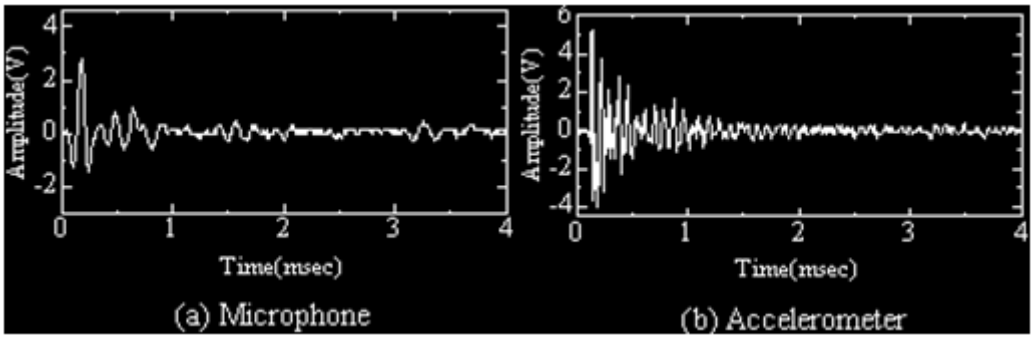

Fig .(6) waveforms (Sound portion).

From **Figure (4) and Figure (5)**, it is obvious that the waveform obtained from sound portion and flaws portion show quite different characteristics. In sound portion, duration of the waveform was shorter than that of flaws ones. On the other hand, waveforms of flaws portion show periodic history curves. With flaws case, both flaws depth is 30 mm and 70 mm, waveforms obtained from microphone and accelerometer show same tendency in terms of periodic history and attenuation characteristics. Tendency of waveforms obtained from FEM analysis show good agreement with experimental ones. In both experimental and analytical results, the greater the diameter of defect, the shorter the period.

Frequency Distribution

Figure (7) Figure(8) show the frequency distributions of impact sounds, surface displacement and analytical results at a depth of 3 and 70 mm for flaws of 200 mm in diameter. For comparison, frequency distribution of sound portion was also shown in Figure 9 (only in experimental data). The figures show elastic wave frequency distributions that have clear single peaks and shapes that are completely different from those in the sound portions **(Figure 9).** Intensities of each spectrum of flaw case were much larger than that of sound one, which is thought to be the characteristics of flaws part. However, in Figure 9 (b), sharp and single peak is also appeared. This is not flexural resonance but longitudinal resonance corresponding to thickness frequency calculated by the following equation.

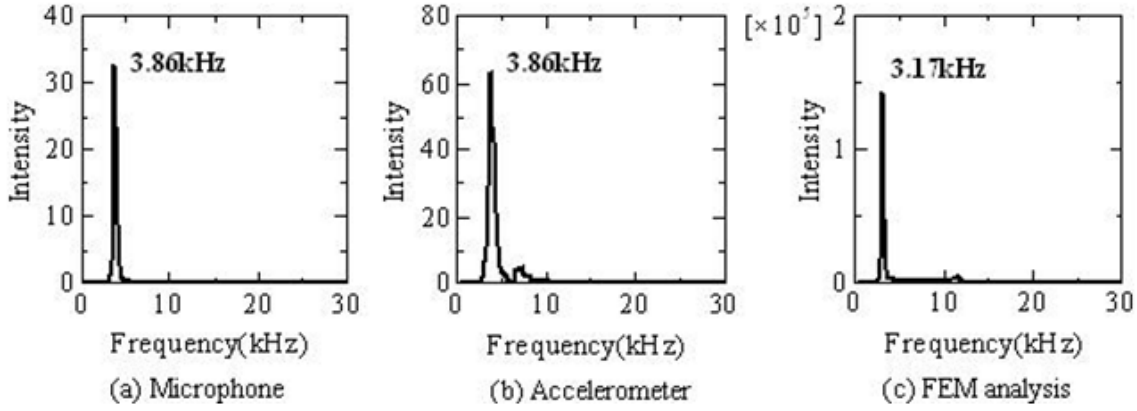

Fig .(7) Frequency distribution (Diameter: 200 mm depth: 30 mm)

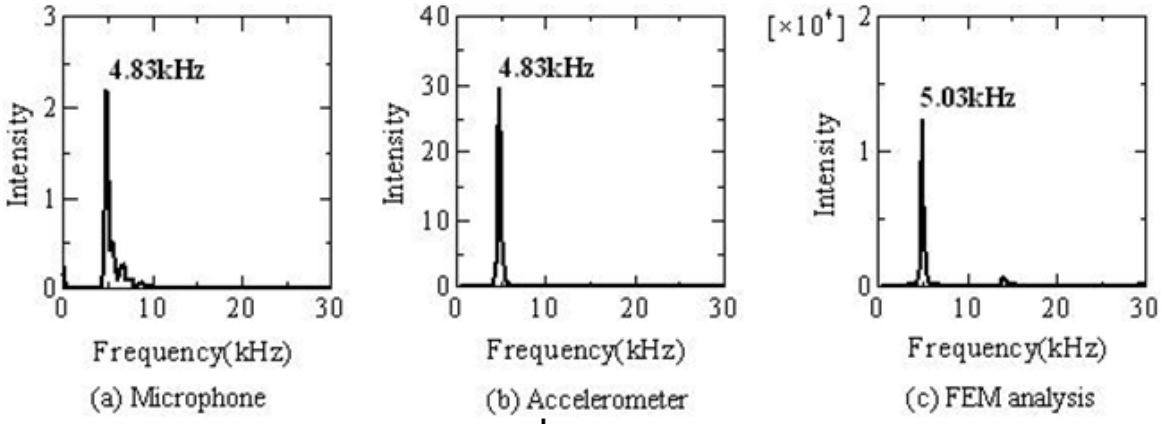

Fig .(8) Frequency distribution (Diameter: 200 mm depth: 70 mm)

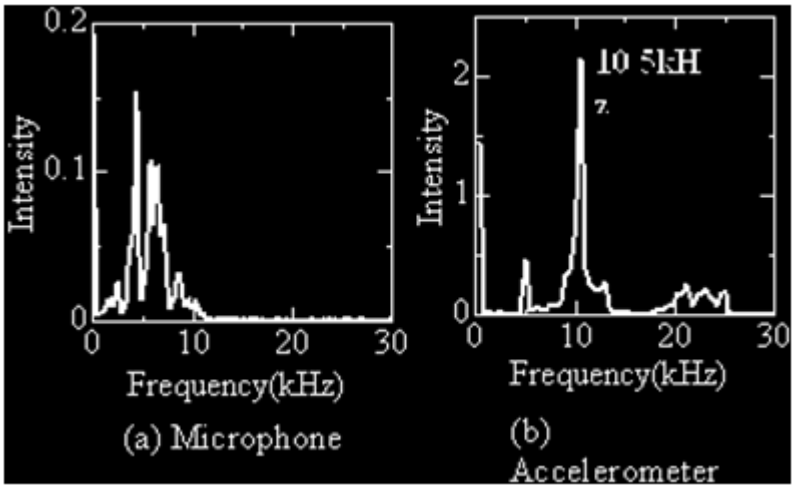

Fig .(9) Frequency distribution (Sound portion)

$$f_t = V / 2T \qquad (3)$$

Where *ft* : thickness frequency(Hz), *V*: elastic wave velocity(m/s) and *T*: concrete thickness(m). In this study, *V* was 4500m/s, *T* was 0.2m. By using the above values, *ft* = 11.25kHz is obtained. This is close to the experimental value. From Figure7 and Figure8, spectral peak obtained from microphone and accelerometer showed similar value. This implies that the phenomena of sound generated by impact and surface displacement was equivalent. The larger the depth of the flaws, the higher the frequency at the peak. This characteristic seems to show that the flaw induced resonance inside the

specimen, which caused spectrum peak of impact sounds to appear. There are good agreements between the experimental and analytical results.

In vibrating disks, the flexural resonance frequency is known to increase as the depth of the disk increases if the disk area is constant [7]. The shift of the spectrum peak described in the above paragraph suggests that the peak component of the spectrum was due to the flexural resonance of the concrete above the defect.

Relation between peak frequency and flaws diameters

Figure (10) and **Figure (11)** show the relation between resonance frequency and flaws diameter obtained from experiment and FEM analysis respectively.

These figures show lower peak frequencies for larger flaws and also show higher peak frequency for deeper flaws. This characteristic can be observed both experiment and analysis. On the other hand, in the analytical results, resonance frequency of 100 mm depth (equal to plate thickness is 100 mm) show lower value than that of 70 mm case except for diameter of flaws are 100, 300, 500mm. This seems to be attributed to the difference between analytical assumption and actual condition of flaws inside the concrete. In analysis, displacement of side in the model was not constrained. However, in experiment, when subjected to impact, the vibration of concrete part upper side of flaws was not separated to around concrete. As a result, flexural resonance was not appeared in the analysis. From **Figure (10) and Figure (11),** under same diameter of flaws, the difference of resonance frequency caused by the increase of flaws depth seems to be small. Taking into consideration of this relation, resonance frequency is thought to be effective index to evaluate the lateral expansion of the flaws inside concrete.

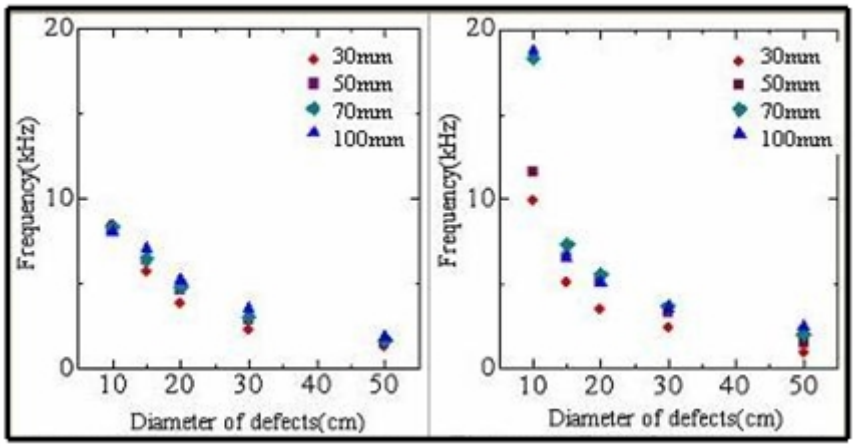

Fig .(10): Peak frequency and defects diameter (Experimental)

Fig .(10) Peak frequency and defects diameter (FEM analysis)

Conclusions

The following conclusions were obtained from this study:

1. Waveforms obtained from experiment and calculated by FEM analysis showed good agreement. So the model used in this study was appropriate.
2. Under the experimental conditions used, the resonance frequencies of the impact sounds and surface displacement mutually agreed in the flaw portions, and they are likely to be equivalent.
3. Frequencies obtained from FEM are also in good agreement with experimental ones.
4. To detect flaws, it is effective to compare the frequency distributions of impact sounds for the defected and sound portions.
5. In this study, it is possible to estimate the size of a flaw using a correlation diagram of resonance frequency and flaw diameter.

References

1. **Nikkei Business Publications, Inc., NIKKEI CONSTRUCTION, No.240, pp.44-45, 1999.9**
2. **Japan Concrete Institute.TC 994: Technical Committee, Committee Report on Nondestructive Evaluation for Diagnosis of Concrete Structures, pp.72-80, 2001**
3. **المواصفات العراقية رقم (5) لسنة 1984 " الاسمنت البورتلندي "، الجهاز المركزي للتقييس والسيطرة النوعية ،بغداد 1984.**
4. **المواصفات العراقية رقم (5) لسنة 1984 " ركام المصادر الطبيعية المستعملة في الخرسانة والبناء "، الجهاز المركزي للتقييس والسيطرة النوعية ،بغداد 1984.**

5. **Sansalone M. J. and Street W. B.t , *Impact Echo*, Bullbrier Press, Ithaca, N. Y. 1997**
6. **Shiratori M., Higai T. and Okamura Y., *"Analytical Study on the Response of Concrete Members for Light Impact Load"*, Proceedings of Japan Concrete Institute, Vol.14, No.1,pp.679-684, 1992**
7. **Ashby M.F. , *Materials Selection in Mechanical Design,* Butterworth-Heinemann, Oxford, 1992**